

CHAPTER V

RESULTS AND DISCUSSION

The deactivation of the adsorbents along with the adsorption process was studied in order to develop the adsorption isotherm and breakthrough model used for the multi-layer adsorber in the natural gas dehydration process. Two types of adsorbents; activated alumina and molecular sieve zeolite type 4A used in natural gas dehydration process, were studied for their adsorption behavior: both static and dynamic along the adsorption process. The deactivation by hydrothermal steaming was employed for deactivating the adsorbents and the effect of deactivated adsorbents on adsorption capacity was then studied in this chapter.

5.1 Adsorbent Preparation for Deactivation

The commercial activated alumina and molecular sieve zeolite 4A were used as the adsorbents in natural gas dehydration process. Because both alumina and molecular sieve zeolite have Al in their structure, exposed to water vapor in natural gas stream and heat in the regeneration step during the adsorption process, the Al in the adsorbent's structure was possibly removed, and this process is known as dealumination.

In 1995, Sano *et al.* reported that the number of water molecules adsorbed on zeolite was associated with the number of alumina in the framework. Thus, when dealumination occurs, the adsorption ability of the adsorbents has to be decreased. Also, the alumina was easily deactivated when applied with heat over 175-300°C (Philip,1995). So, the decreased of the adsorption capacity during the adsorption process was mainly considered as hydrothermal deactivation.

In this work, the activated alumina and molecular sieve zeolite were deactivated by the hydrothermal steaming process. The percentage of deactivation was analyzed by laboratory techniques such as surface area analysis, average crystal size analysis, adsorption capacity analysis, and crystallinity analysis.

5.2 Adsorbent Characterization

The adsorption behavior of the fresh and the deactivated adsorbents prepared by hydrothermal steaming can be different. In order to develop the mathematical model for water vapor adsorption, the characteristics of the adsorbents was therefore characterized for their physical properties and deactivation percentages.

5.2.1 Fresh Adsorbent Characterization

The static adsorption capacity, crystal structure, specific surface area, and XRD patterns of fresh adsorbents are discussed in this part.

5.2.1.1 Static Adsorption Capacity of Fresh Adsorbents

Alumina and molecular sieve kept in saturated water vapor (100%RH) at 25°C and 1 atm was determined the static adsorption capacity by using TG/DTA equipment. The adsorption capacity was determined in the temperature range between 30 to 350°C because the major water desorption is occurred in this range. The static adsorption capacities of fresh adsorbents are shown in Table 5.1 below.

Table 5.1 Static adsorption capacity of fresh adsorbents at 100%RH and 25°C

Adsorbent	Adsorption capacity*	Adsorption capacity**	Adsorption capacity (%)
Alumina	29.94	-	28.00
Mol siv(1/8")	20.37	22.0	17.22
Mol siv(1/16")	21.39	22.0	18.37

* Adsorption capacity (mg of water vapor/lg of adsorbent) measured in the TG/DTA range from 30 to 350°C

** UOP specification (mg of water vapor/lg of adsorbent) at 25°C and 17.5 mmHg

Desorption of water molecules from the molecular sieve zeolites of size 1/8" and 1/16" occurs in two steps as shown in Figure 5.1. The first desorption step was around 30 to 70°C, and the second one was around 90 to 250°C. This is because the water is adsorbed on the macro-pores and macro-pores within the zeolite crystals.

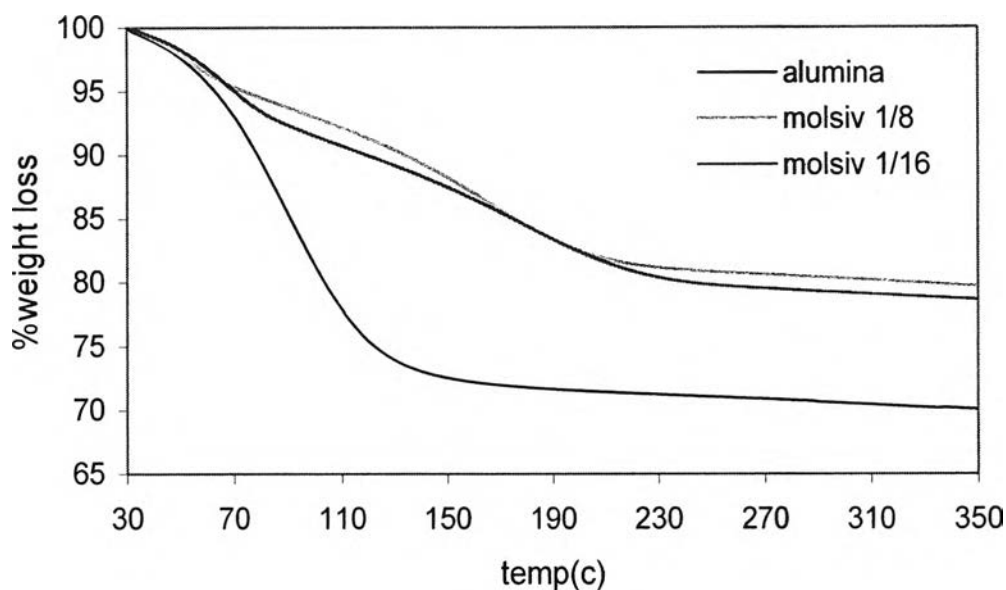


Figure 5.1 Weight loss of water saturated on fresh adsorbents from TG/DTA experiments.

Also, from Figure 5.1, it was found that the adsorption capacity of alumina was higher than that of molecular sieve because multilayer adsorption of water can occur on activated alumina possessing only macro-pores. On the other hand, for the molecular sieve zeolites, most of surface area contributing to water adsorption is in the macro-pores, which allows only monolayer adsorption to occur. Between the two sites of zeolites, the size 1/8" had slightly less adsorption capacity than the size 1/16". Also, desorption continues decreasing very slowly due to little amount of water remaining in the pores at the temperatures over 250°C. Therefore, this implies that the temperature required to effectively regenerate the molecular sieve zeolite should be above 250°C or higher.

In addition, the adsorption strength can be determined from the TGA results by considering the weight-loss-derivative of each adsorbent. This derivative curves give the desorption temperatures as shown in Table 5.2, and the temperature indicates the adsorption strength of each adsorbent. Therefore, although activated alumina has higher adsorption capacity, it has weaker adsorption strength when compared to the molecular sieve zeolite because the structure of activated alumina offers lesser affinity due to lesser polarity than the molecular sieve zeolite.

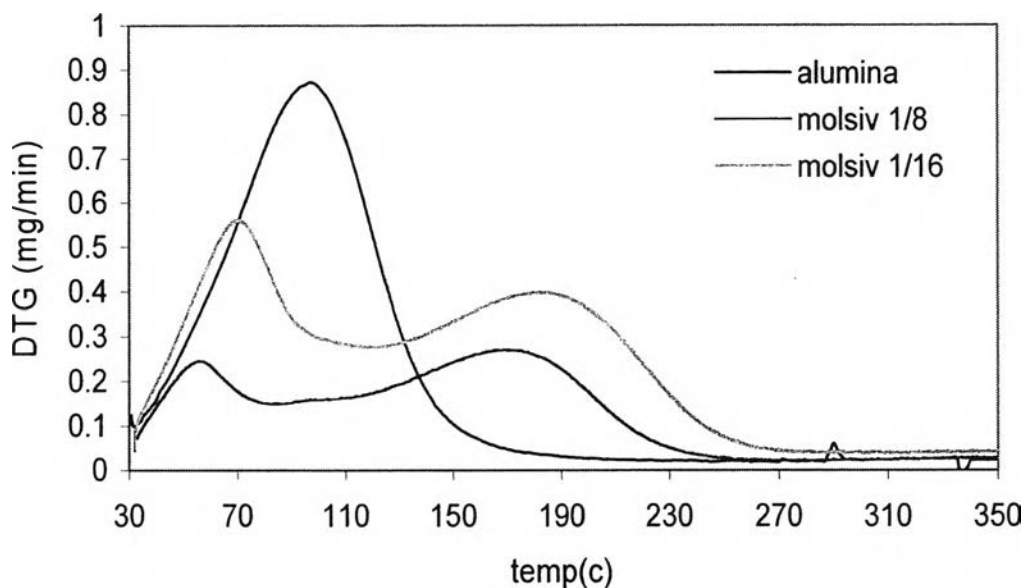


Figure 5.2 Weight loss derivative of water saturated on fresh adsorbents from TG/DTA experiments.

The curves in Figure 5.2 exhibits two derivative peaks at the temperatures around 54 to 70°C and 176 to 189°C, because the water adsorbed in both macro-pores and micro-pores within the zeolite crystals. Therefore, at the temperatures over 350°C, it can be implied that the adsorbents could already deactivate. Therefore, in this work, temperature and aging time were varied in order to produce the deactivated adsorbents.

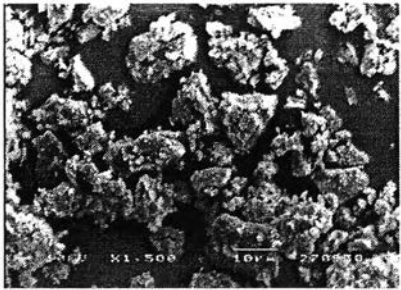
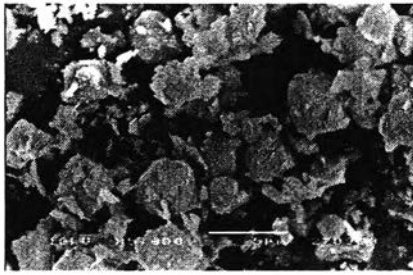
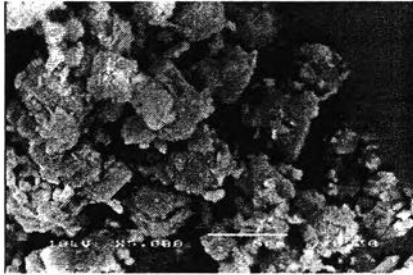
Table 5.2 Desorption temperature of fresh adsorbents at 100%RH and 25°C

Adsorbent	Desorption temperature(°C)	
Alumina	98	
	Macro-pore	Micro-pore
Molsiv (1/8")	54	176
Molsiv (1/16")	70	189

5.2.1.2 Scanning Electron Microscopy of Fresh Adsorbents

Scanning Electron Microscopy (SEM) was used to determine the surface morphology and crystal size of the adsorbents. The change of the particle size can also be determined. Fresh adsorbents were analyzed and compared to the deactivated adsorbents. The SEM analysis results of fresh adsorbents are shown in Table 5.3 below.

Table 5.3 Scanning Electron microscopy images of fresh adsorbents

Sample	SEM images
Alumina	 <p data-bbox="1044 1084 1135 1118">×1500</p>
Mol siv (1/8")	 <p data-bbox="1044 1401 1135 1435">×3500</p>
Mol siv (1/16")	 <p data-bbox="1044 1714 1135 1748">×3500</p>

The SEM images show the morphology of each adsorbent. Alumina is an amorphous material, whereas the molecular sieve zeolite having the basis LTA structure shows the crystals with a cubic shape. Therefore, the particles sizes distribution of the molecular sieve zeolite can be determined from SEM images.

The size distribution plot of molecular sieve zeolite of size 1/8" and 1/16" are shown in Figures 5.3 and 5.4 below. The data for size distribution plots are shown in Appendix D.

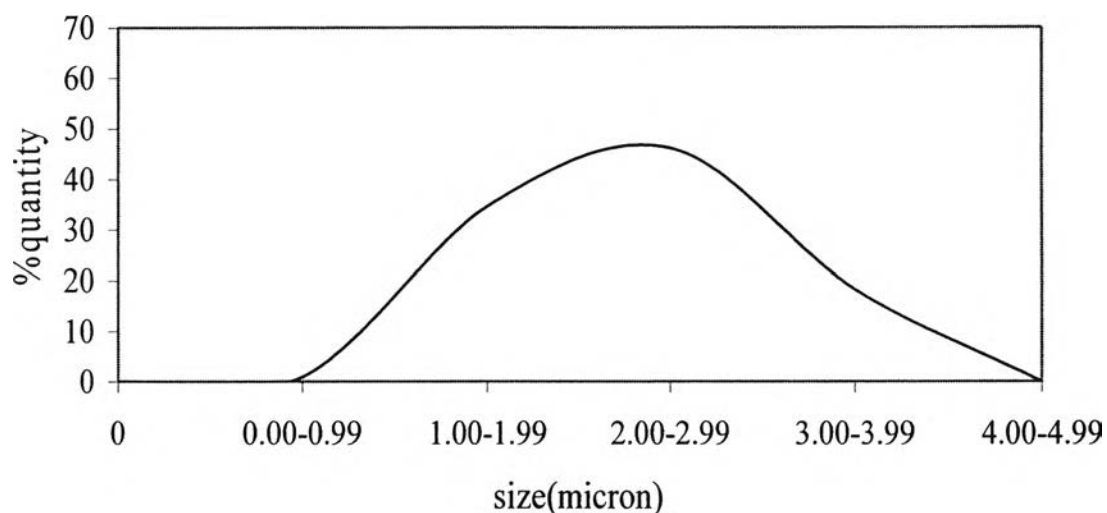


Figure 5.3 The size distribution of molecular sieve zeolite of size 1/8".

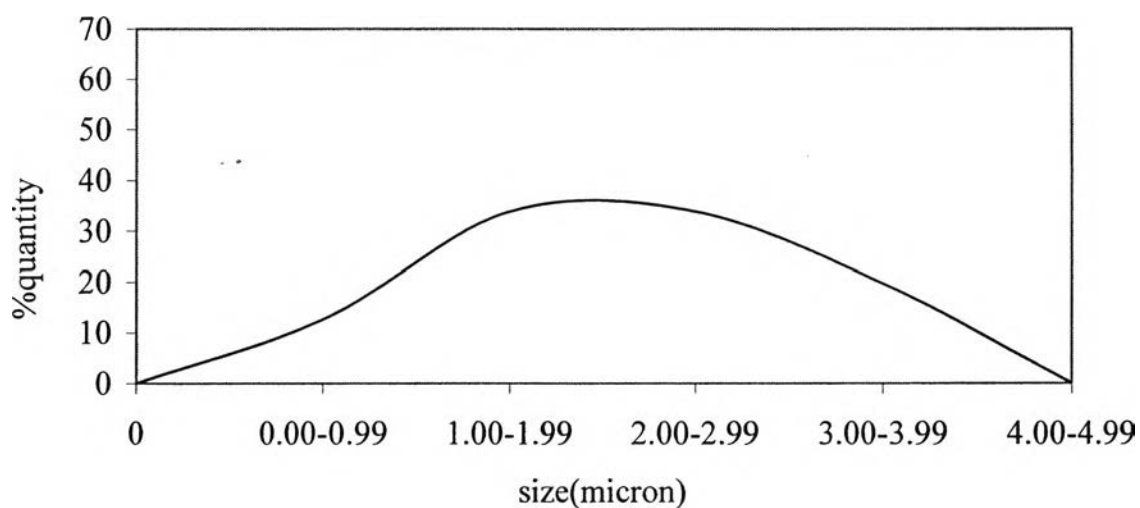


Figure 5.4 The size distribution of molecular sieve zeolite of size 1/16".

The mean particle size of the 1/8" molecular sieve adsorbent calculated from the plot is about 2.31 microns and 2.10 microns for the 1/16" molecular sieve zeolite.

5.2.1.3 Surface Area of Fresh adsorbents

The high surface area materials are needed for the adsorption process in order to adsorb a high amount of the adsorbate onto the adsorbent. Thereby, in this work the surface area was determined using the BET method, using the Sorptomatic 1990 equipped version 1.02, for both fresh and deactivated adsorbents. The surface areas of the adsorbents reported in the literature are listed in Table 5.4.

Table 5.4 Surface area of the general commercial adsorbents*

Adsorbent	Surface area (m ² /g)
Activated Alumina	50 - 250
Molecular Sieve Zeolite	800 - 1000

* Philip, (1995)

Due to the limitation of the molecular sieve zeolite 4A itself, which has very narrow pore size, N₂ gas can hardly pass through the zeolite pores and adsorb onto the pore surface. The specific surface area, pore volume, and monolayer volume of activated alumina are only reported. The specific surface area, pore volume, and monolayer volume of fresh alumina adsorbent are shown in Table 5.5.

Table 5.5 The specific surface area, pore volume, and monolayer volume of fresh activated alumina from BET analysis

Value	Results
Specific surface area (m ² /g)	200.2
Pore specific volume(cm ³ /g)	0.492
Monolayer volume (cm ³ /g)	45.98

5.2.1.4 X-RAY Diffraction Patterns of Fresh Adsorbents

The XRD diffraction pattern of activated alumina and molecular sieve zeolite of size 1/8" and 1/16" were obtained by the Rikagu (RINT-2200) XRD machine. The samples were scanned from 3 degree to 90 degrees (2θ)

with the scanning speed of 0.02 degrees/min, and the results for alumina and molecular sieve zeolite of size 1/8" and 1/16" are shown in Figures 5.5 to 5.7, respectively.

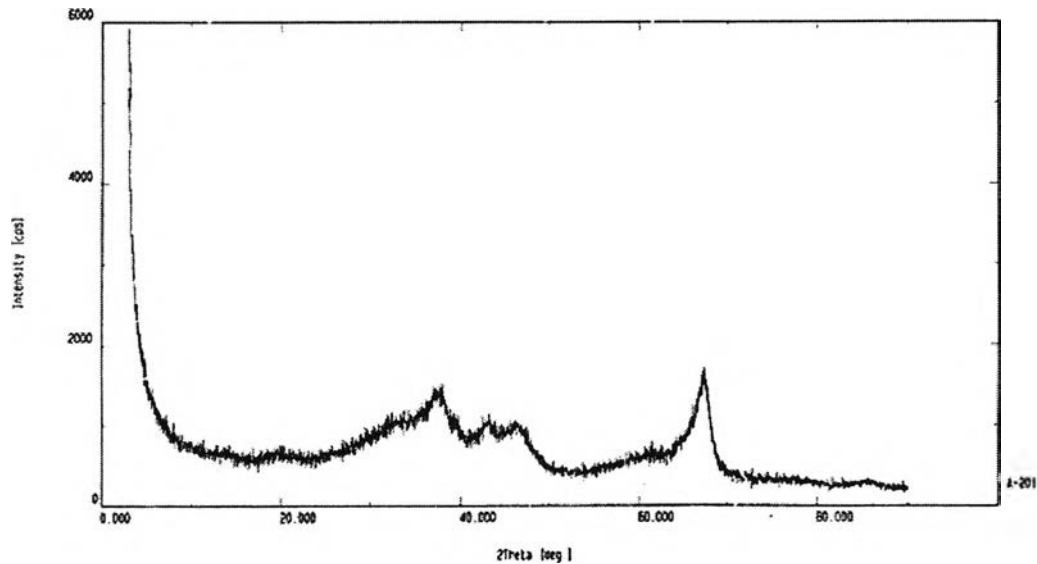


Figure 5.5 X-Ray Diffraction pattern of fresh activated alumina.

The XRD pattern of fresh activated alumina, Figure 5.5, shows the broad peak which indicates an amorphous solid structure whereas the XRD patterns of molecular sieve zeolites, Figures 5.6 and 5.7 represent highly crystalline structures.

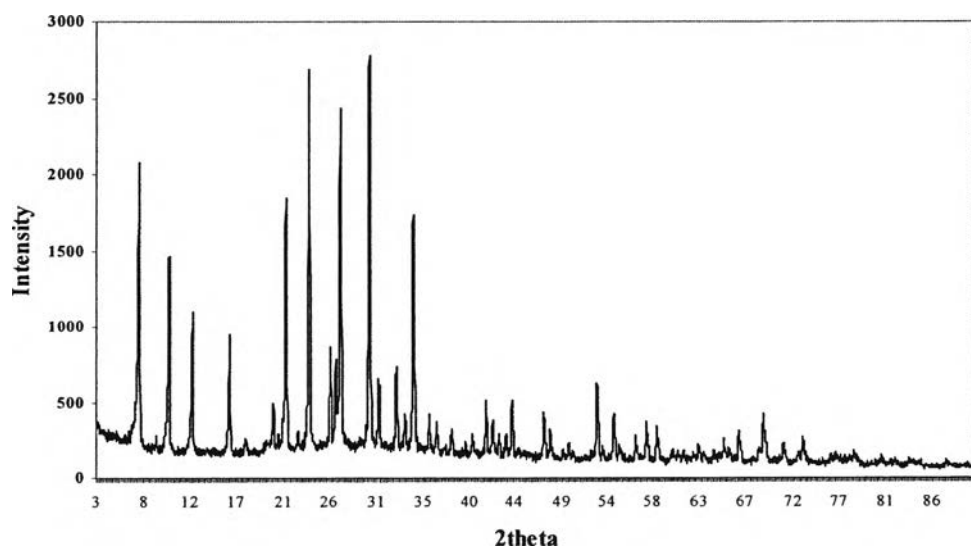


Figure 5.6 X-Ray Diffraction pattern of fresh molecular sieve zeolite of size 1/8".

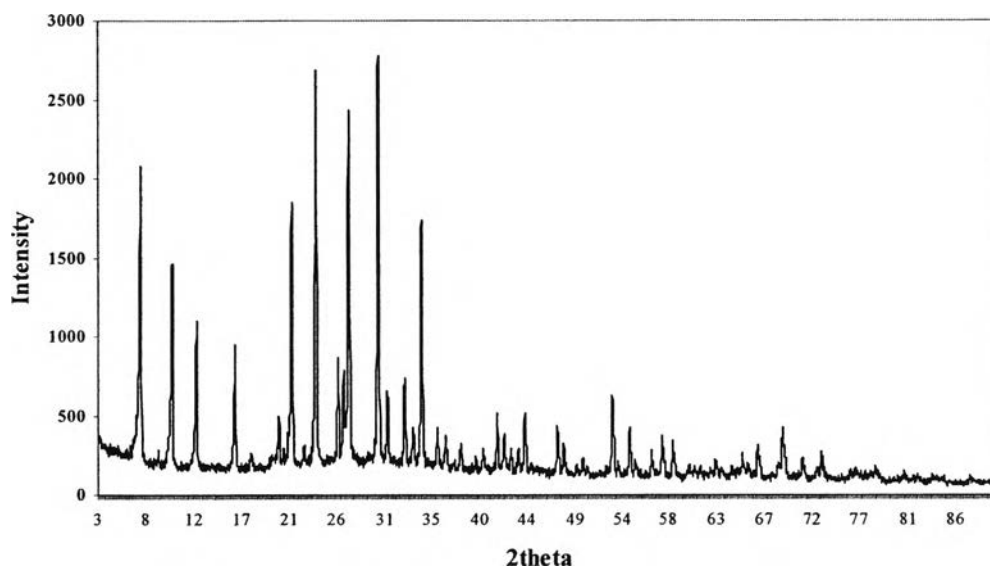


Figure 5.7 X-Ray Diffraction pattern of fresh molecular sieve zeolite of size 1/16”.

5.2.2 Deactivated Adsorbent Characterization

The activated alumina and molecular sieve zeolite were deactivated by the hydrothermal steaming process as discussed before. Temperature and aging time were varied to achieve several deactivation percentages. The apparatus was setup for this part, which was composed of a rotameter to adjust the nitrogen purge gas into the system, a heater with temperature controller to provide high temperature, a steam generator or heating mantle to give saturated steam at atmospheric pressure, and an aging reactor which allows purging gas and steam to pass through the adsorbent inside. The flow rate of the steam was fixed at about 30 ml/min, but the aging time and heating temperature were varied to obtain a series of deactivated adsorbents with different degrees of deactivation. Finally, the deactivated adsorbents were characterized for their adsorption and physical properties.

5.2.2.1 *Deactivated Alumina Characterization*

Since the activated alumina was used as an adsorbent, the physical properties changed by hydrothermal steaming were studied. Generally, a high surface area material is required for use as an adsorbent, so the change of specific surface area was studied. Not only is surface area important for adsorption, but also the structural component can affect the adsorption capacity. Therefore, the XRD and SEM analysis was studied.

A. Static Adsorption Capacity of Deactivated Alumina

The static adsorption capacity of water vapor adsorbed on alumina at 25°C, 1atm was examined. The results in Table 5.6 show the decrease of static adsorption capacity up to 88.30% along with an increase of aging severity.

Table 5.6 The adsorption capacity analysis of fresh and deactivated alumina

Condition	Adsorption capacity* (g water/100g adsorbent)	%loss of adsorption capacity
Fresh	25.65	0.00
300°C 1day	14.76	42.46
400°C 2days	8.23	67.92
550°C 1day	5.65	77.97
550°C 2days	3.00	88.30

* The adsorption capacity determined at 25°C and 40%RH.

B. Specific Surface Area of Deactivated Alumina

The change of specific surface of deactivated alumina was examined by the BET method and found to be decreased by hydrothermal steaming as shown in Table 5.7.

Table 5.7 The specific surface area analysis of fresh and deactivated alumina

Condition	Specific Surface Area* (m ² /g)	%loss of specific surface area
Fresh	200.2	0.00
300°C 1day	190.4	4.89
400°C 1day	185.1	7.52
400°C 2days	172.9	13.61
400°C 3days	164.8	17.67
500°C 1day	154.1	22.99
500°C 2days	144.1	28.00
550°C 1day	130.0	35.05
550°C 2days	124.0	38.05

* BET Method.

Since the adsorption of water vapor on alumina depends on both chemisorption and physisorption on its surface, the adsorption behavior related to the change of surface area of deactivated alumina was studied. The specific surface area and the adsorption capacity of the activated alumina at several aging conditions are shown in Figure 5.8. The plot indicates that the adsorption capacity decreases linearly with the decrease of specific surface area. Because Al, which is the active site on alumina surface, was lost, the water molecules can hardly to adsorb on the surface of the alumina.

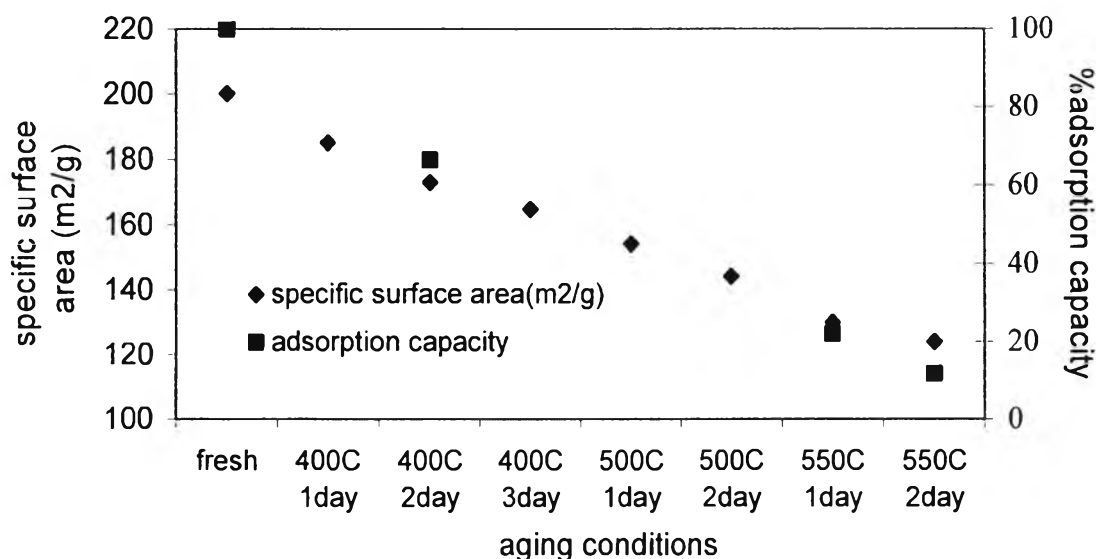


Figure 5.8 Specific surface area and the adsorption capacity of the activated alumina at several aging conditions.

In addition, the relationship between the loss of adsorption capacity and the loss of specific surface area in Figure 5.9 indicates the adsorption capacity rapidly decreases with the surface area reduction up to about 15%, but after the alumina loses its surface area over 15%, the loss of adsorption capacity was slightly decreased. This relationship can be explained by the power law relation, $y = 28.29x^{0.3034}$ where x is % loss of adsorption capacity, and y is % loss of surface area, respectively.

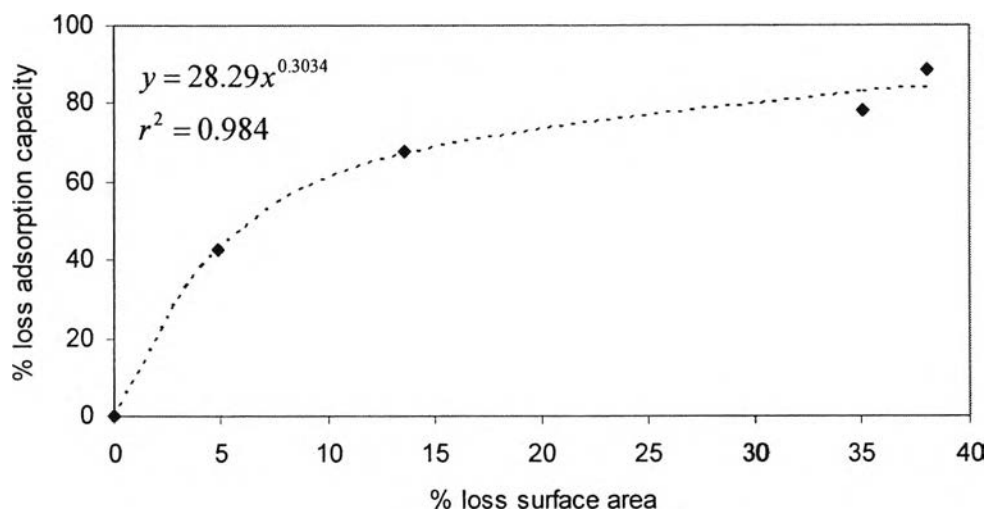


Figure 5.9 Relationship between the loss of adsorption capacity and the reduction of specific surface area of deactivated alumina.

C. Scanning Electron Microscopy of Deactivated Alumina

The images from Scanning Electron Microscopy (SEM) give the basic morphology. Since alumina has amorphous structure, the crystal size could not be determined from the SEM images. Also, SEM images in Table 5.7 show no significant change upon the current degree of deactivation, so the percentages of deactivation in terms of crystal size reduction can not be determined.

D. X-Ray Diffraction Patterns of Deactivated Alumina

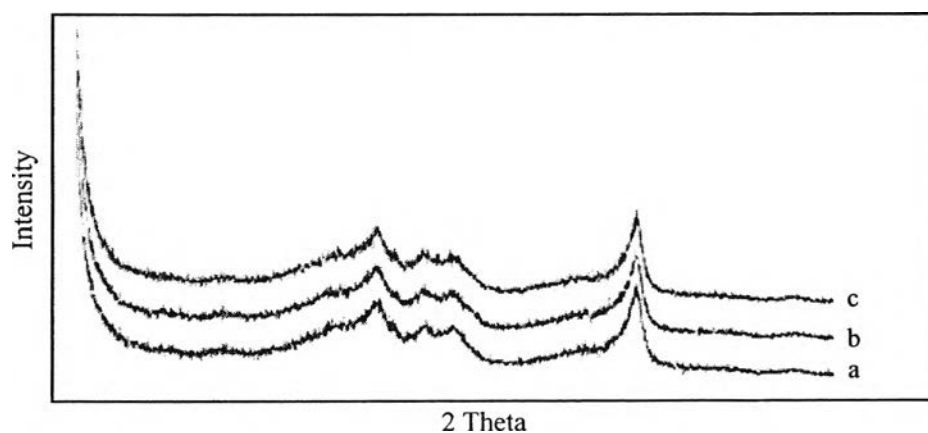
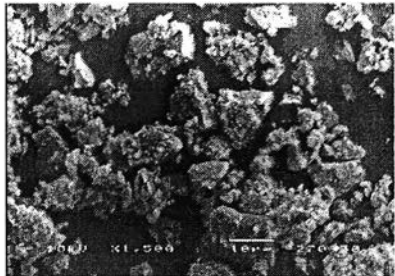
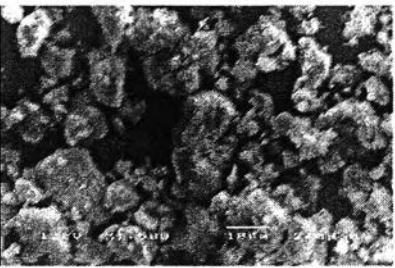
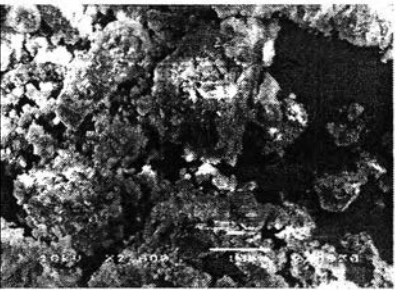
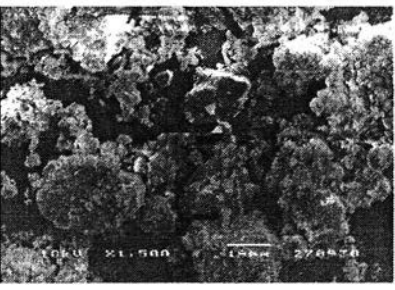


Figure 5.10 The XRD patterns of fresh alumina: (a) fresh, (b) 67.92% deactivation, and (c) 88.30% deactivation.

The XRD patterns of deactivated alumina in Figure 5.10 show amorphous structure similar to that of fresh alumina. The unchanged patterns mean that the morphology was still remained while the adsorption capacity decreases.

Table 5.8 Scanning Electron microscopy images of activated alumina at several deactivation conditions

Sample	SEM images
Fresh	 ×1500
400°C 1 day aging	 ×1500
550°C 2 days aging	 ×1500
550°C 3 days aging	 ×1500

5.2.2.2 Deactivated Molecular Sieve Zeolite Characterization

The molecular sieve zeolite of size 1/8" and 1/16" were deactivated by severe hydrothermal steaming, and the number of aging batches was varied to obtain several deactivation percentages. Also the degree of deactivation was determined using several laboratory techniques for analysis of average crystal size, adsorption capacity, and crystallinity.

A. Static Adsorption Capacity of Deactivated Molecular Sieve Zeolite

The adsorption capacities of the adsorbents aged at several conditions were examined at 25°C and 40%RH, and the results are shown in Table 5.9. It is found that the adsorption capacity of deactivated molecular sieve zeolite decreases when hydrothermally aged with more severe conditions. It means the presence of both water vapor and high temperature in the natural gas adsorber can make the molecular sieve adsorbent packed inside lose its adsorption ability.

Table 5.9 Adsorption capacity at several aging conditions and percentages of deactivation described by the loss of adsorption capacity

Deactivation Conditions	Molsiv (1/8")		Molsiv (1/16")	
	Adsorption capacity*	%deactivation**	Adsorption capacity*	%deactivation**
Fresh	18.50	0.00	19.00	0.00
40 batches	16.50	10.81	-	-
70 batches	-	-	17.90	5.79
120 batches	15.70	15.13	16.32	14.10

* The adsorption capacity (g water/100 g adsorbent) obtained at 25°C and 40%RH.

** The deactivation due to loss of adsorption capacity.

B. Specific Surface Area of Deactivated Molecular Sieve Zeolite

The specific surface area of molecular sieve zeolite can not be determined using the machine in the College. N₂ gas hardly adsorbs into the pore of 4A zeolite because the pore size of 4A zeolite is about 4 angstroms and the kinematics diameter of N₂ is about 3.6 angstroms. N₂ therefore, can hardly get into the zeolite pores. In addition, the surface area analyzer, Sorptomatic, can not

accommodate low pressure enough to make the N₂ gas diffuse into the zeolite 4A pores. Thus, the specific surface area of the molecular sieve zeolite will not be reported in this part.

C. Average Crystal Size of Deactivated Molecular Sieve Zeolite from SEM Images

The data of average crystal size were determined from the SEM images, and the average crystal size distribution as shown in Appendix E. The percentages of deactivation due to the loss of average crystal size are shown in Table 5.10.

Table 5.10 Average crystal size of molecular sieve zeolite and the %deactivation at several aging conditions

Condition	Molsiv (1/8")		Molsiv (1/16")	
	Average crystal size* (micron)	%size reduction**	Average crystal size* (micron)	%size reduction**
Fresh	2.31	0.00	2.10	0.00
10 batches	2.04	11.7	2.09	0.72
20 batches	1.86	19.4	2.01	4.40
30 batches	1.78	23.2	1.72	18.0
40 batches	1.53	33.8	1.65	21.3
50 batches	1.27	45.0	1.62	23.0
60 batches	1.17	49.4	1.33	36.8
70 batches	1.17	49.5	1.11	47.1
80 batches	1.13	51.0	1.10	47.9
90 batches	1.10	52.3	1.03	51.1
100 batches	1.09	52.5	1.00	52.4
120 batches	1.06	54.0	0.98	53.2

* determined by SEM analysis

** %deactivation due to loss of average crystal size

The SEM images and size distribution plots show the change of average crystal size of molecular sieve zeolite upon deactivation. Figures 5.11 and 5.12 show the adsorption capacity and the average crystal size of the deactivated molecular sieve zeolite of size 1/8" and 1/16", respectively. The plots show the

decrease of the adsorption capacity with the average crystal size at various aging temperatures and time.

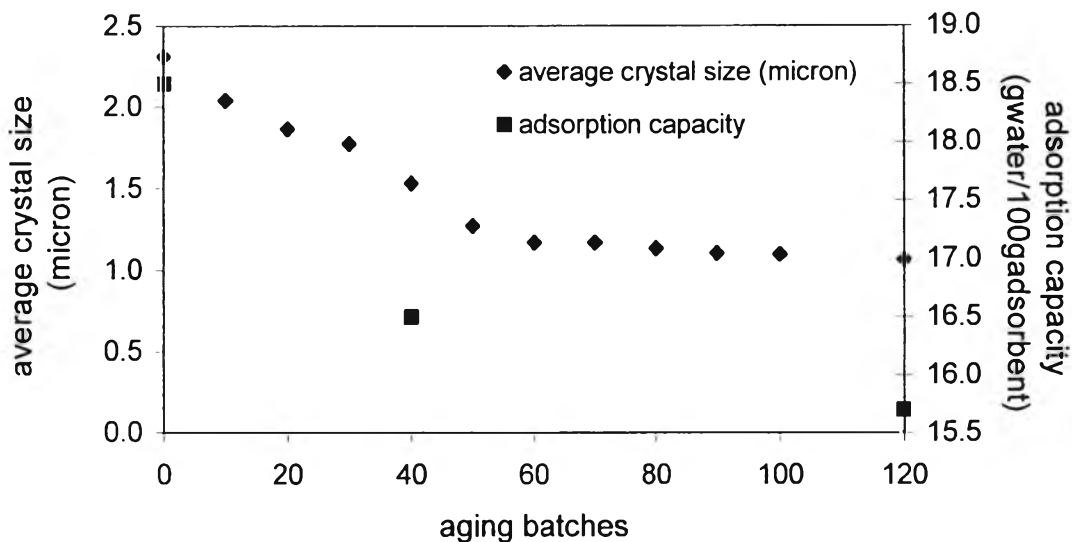


Figure 5.11 Adsorption capacity and the average crystal size of the deactivated 1/8" molecular sieve zeolite at various numbers of batches.

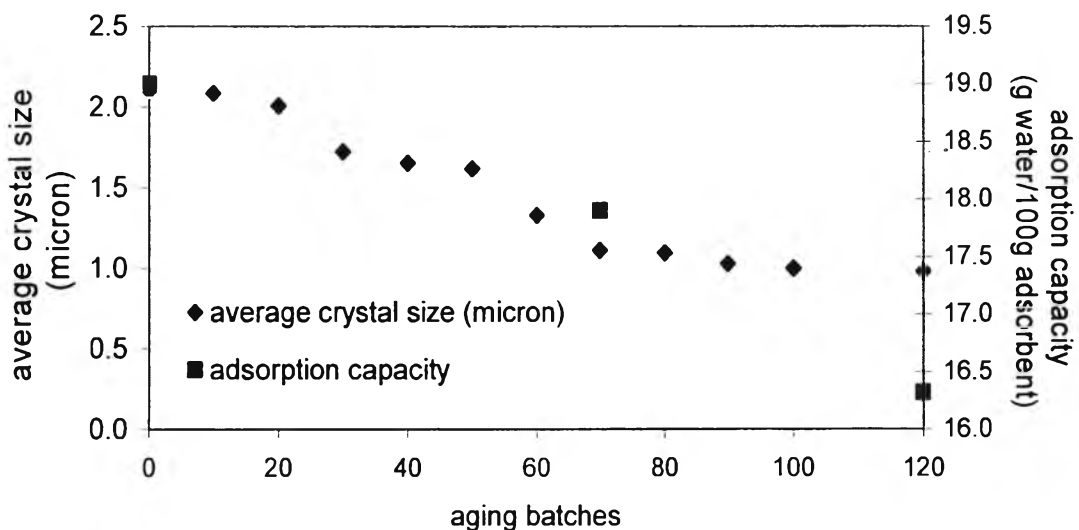


Figure 5.12 Adsorption capacity and the average crystal size of the deactivated 1/16" molecular sieve zeolite at various numbers of batches.

In addition, the plot in Figure 5.13 indicates the linear relationship between the loss of average crystal size and the loss of adsorption capacity of 1/8" molecular sieve zeolite, which can be explained by the

equation $y = 0.2922x$, where x is % reduction of average crystal size and y is % loss of adsorption capacity. The plot of molecular sieve zeolite of size 1/16" illustrates the exponential relationship, $y = 0.0063e^{0.1450x}$ where x is % reduction of average crystal size and y is % loss of adsorption capacity as shown in Figure 5.14.

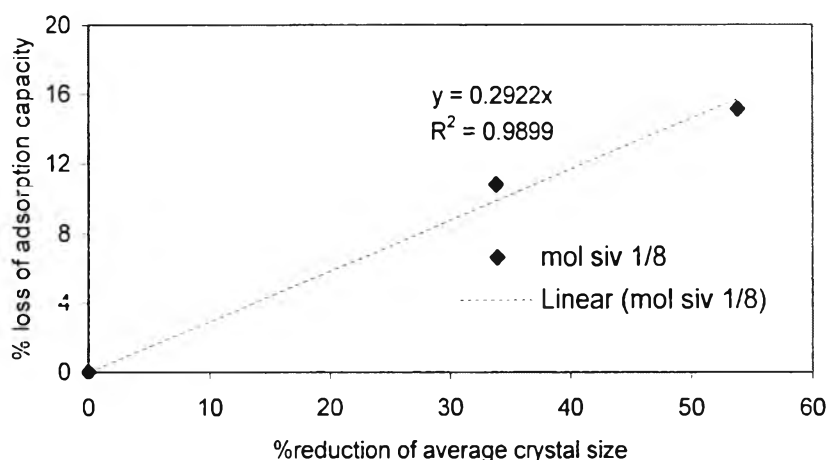


Figure 5.13 The relationship of the loss of adsorption capacity and the reduction of average crystal size of 1/8" molecular sieve zeolite.

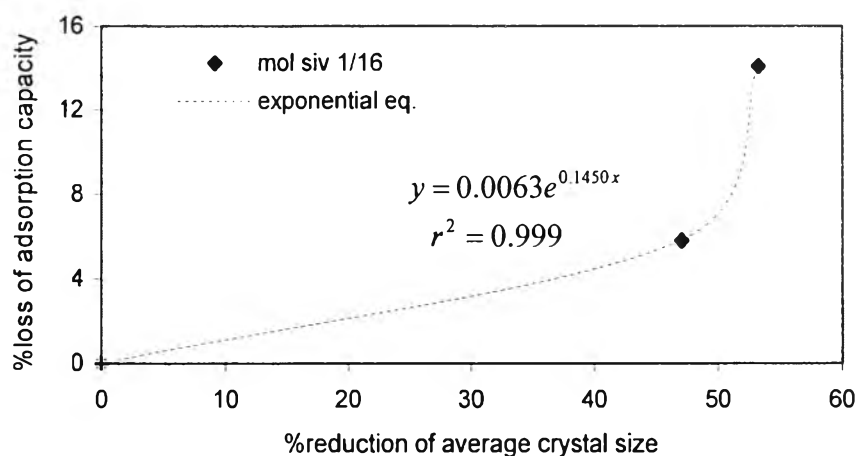


Figure 5.14 The relationship of the loss of adsorption capacity and the reduction of average crystal size of 1/16" molecular sieve zeolite.

D. X-Ray Diffraction Patterns of Deactivated Molecular Sieve Zeolite

The XRD patterns of deactivated molecular sieve zeolite of size 1/8" and size 1/16" are shown in Figures 5.15 and 5.16, respectively. "Deactivation" for the molecular sieve is hereby defined as the loss in adsorption

capacity. The XRD patterns illustrate a high crystalline structure. The similar patterns of fresh and deactivated zeolites mean that the crystallinity is still remained while the adsorption capacity decreases.

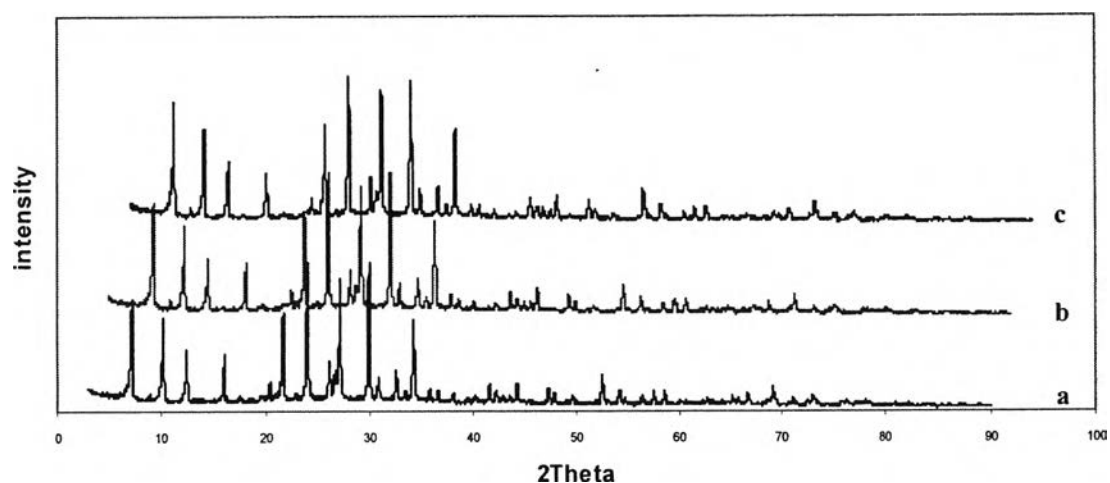


Figure 5.15 The XRD patterns of 1/8" Molecular sieve: (a) fresh, (b) 10.81% deactivation, and (c) 15.13% deactivation.

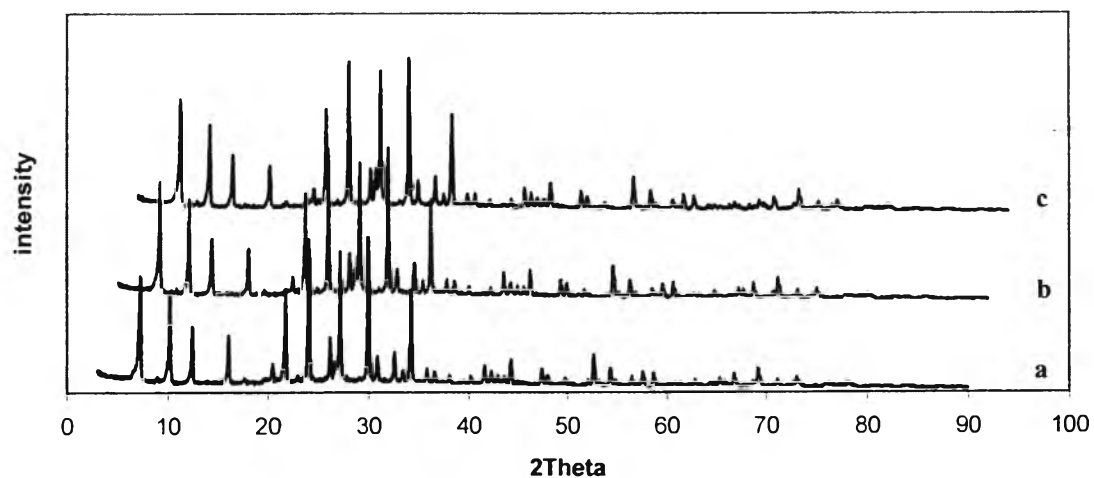


Figure 5.16 The XRD patterns of 1/16" Molecular sieve: (a) fresh, (b) 5.79% deactivation, and (c) 14.10% deactivation.

5.3 Equilibrium Adsorption Isotherm Development

The water adsorption on the adsorbents packed in the stainless adsorber of 22.7 ml was performed at several relative humidity levels, and the equilibrium adsorption isotherms of fresh and deactivated adsorbents were determined in this part. The adsorption isotherms were developed at 25°C and 1 atm using the apparatus set up by Chaikasetpaiboon (2002) and Uttamaroop (2003). The conditions used in the experiments were obtained from calculation as shown in Appendix C. The equilibrium water adsorption was performed at several relative humidity levels.

5.3.1 The Equilibrium Adsorption Isotherm of Fresh Adsorbents

5.3.1.1 *Fresh Alumina*

The equilibrium adsorption isotherm of fresh alumina indicates almost linear relationship between the relative humidity and adsorption capacity. This means water vapor adsorbs as the n-layer or multilayer adsorption. The adsorption isotherm is well fitted with a Freundlich isotherm ($q^* = ac^b$), which parameter a is 1.195 and b is 0.8313. The result is shown in Figure 5.17.

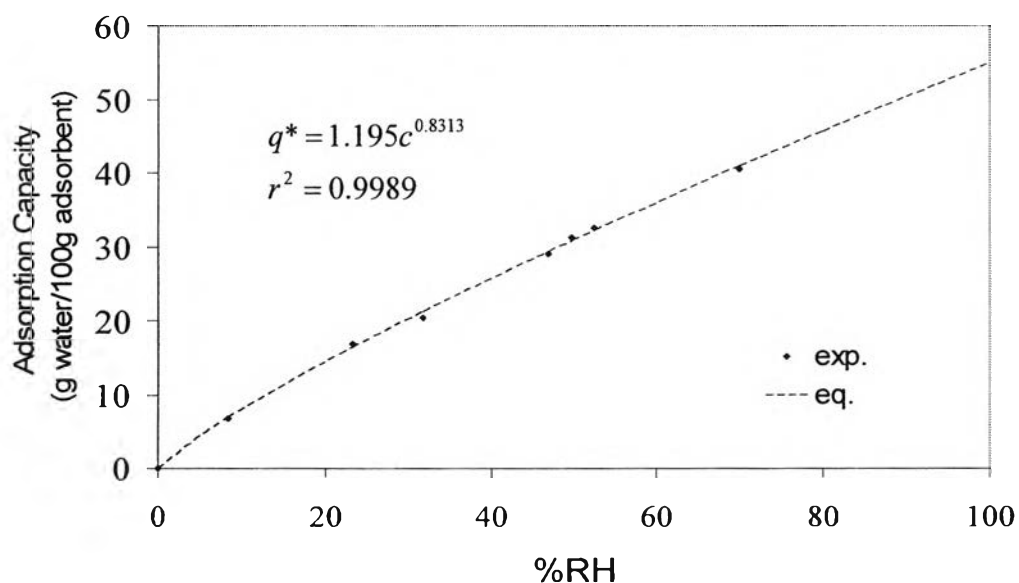


Figure 5.17 Adsorption Isotherm of fresh alumina.

5.3.1.2 *Fresh Molecular Sieve Zeolite*

The equilibrium adsorption isotherms of fresh molecular sieve are fitted well using the Aranovich and Donohue (A-D) equations (Aranovich, 1995),

which covers the multilayer adsorption after complete monolayer adsorption. Aranovich and Donohue proposed the isotherm model of the following form:

$$q = \frac{q_m f(P)}{\left(1 - \frac{P}{P_s}\right)^d}$$

Here, q is the adsorbed moles, and the term $1/(1 - P/P_s)^d$ describes the singularity. Given the definition of $f(P)$, the monolayer capacity q_m can be determined as $f(P_s)$ because $f(P_s)$ corresponds to the maximum monolayer adsorption. Then, Langmuir, Toth, UNILAN, or Sips equation can be substituted in $f(P)$ of the A-D equation.

A. Fresh 1/8" Molecular Sieve Zeolite

The equilibrium adsorption isotherm of 1/8" molecular sieve zeolite obtained from the experiment shows the s-shape curve similar to Type II Brunauer, which water vapor completes monolayer adsorption at around 17.5 g water /100g of adsorbent (9.72 mol/kg) and then starts the multilayer adsorption at high relative humidity as shown in Figure 5.18. Although, the ordinary Langmuir and BET isotherms are fitted with the experimental isotherm data, but the r^2 from the A-D with Toth equation indicates the most accurate result as shown in Table 5.11.

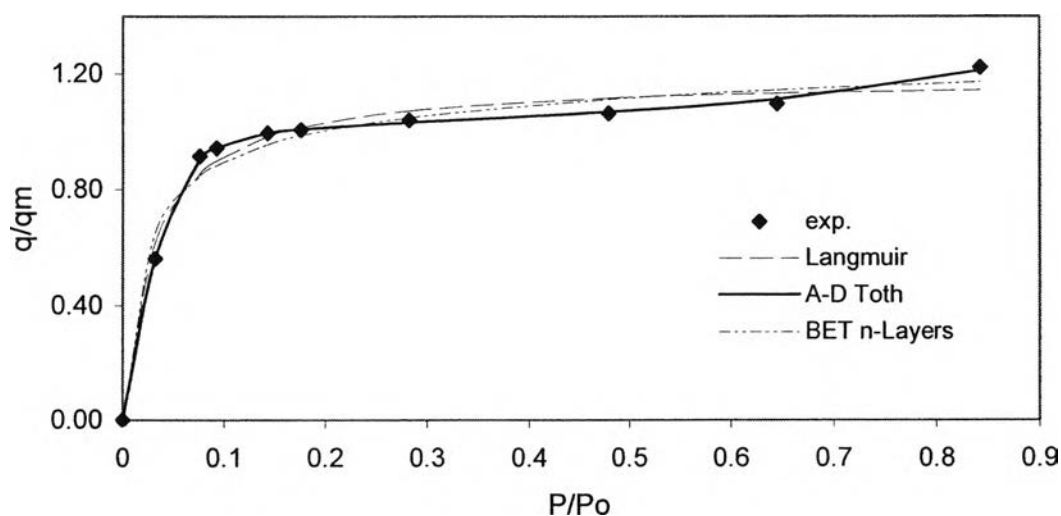


Figure 5.18 Equilibrium adsorption isotherm of fresh 1/8" molecular sieve zeolite.

Table 5.11 Comparison of the equilibrium adsorption isotherm equations for fresh molecular sieve zeolite of size 1/8''

Equation	Equilibrium adsorption isotherm equation [†]
Langmuir	$q^* = \frac{q}{q_m} = \frac{7.083c}{1 + 0.3414c}, r^2 = 0.983$
A-D for Toth	$q^* = \frac{q}{q_m} = \frac{P}{(4.575 \times 10^9 + P^{1.971})^{1/1.971} (1 - P/P_s)^{0.1042}}, r^2 = 0.998$
BET for n-Layers	$q^* = \frac{q}{q_m} = \left[\frac{53.3435(P/P_s)}{1 - (P/P_s)} \right] \left[\frac{1 - (1.4121 + 1)(P/P_s)^{1.4121} + 1.4121(P/P_s)^{1.4121+1}}{1 + (53.3435 - 1)(P/P_s) - 53.3435(P/P_s)^{(1.4121+1)}} \right], r^2 = 0.979$

[†] q = moles adsorbed, q_m = moles adsorbed at complete monolayer, c = concentration (mol/l), P = pressure (kPa), P_s = saturated pressure (kPa)

B. Fresh 1/16'' Molecular Sieve Zeolite

The equilibrium adsorption isotherm of 1/16'' molecular sieve zeolite is similar in shape to 1/8'' molecular sieve zeolite as shown in Figure 5.19, and the isotherm for 1/8'' molecular sieve zeolite can therefore be applied for 1/16'' molecular sieve zeolite. The complete monolayer coverage from the experiment is about 17.7 g of water /100g of adsorbent, or 9.83 mol/kg of adsorbent.

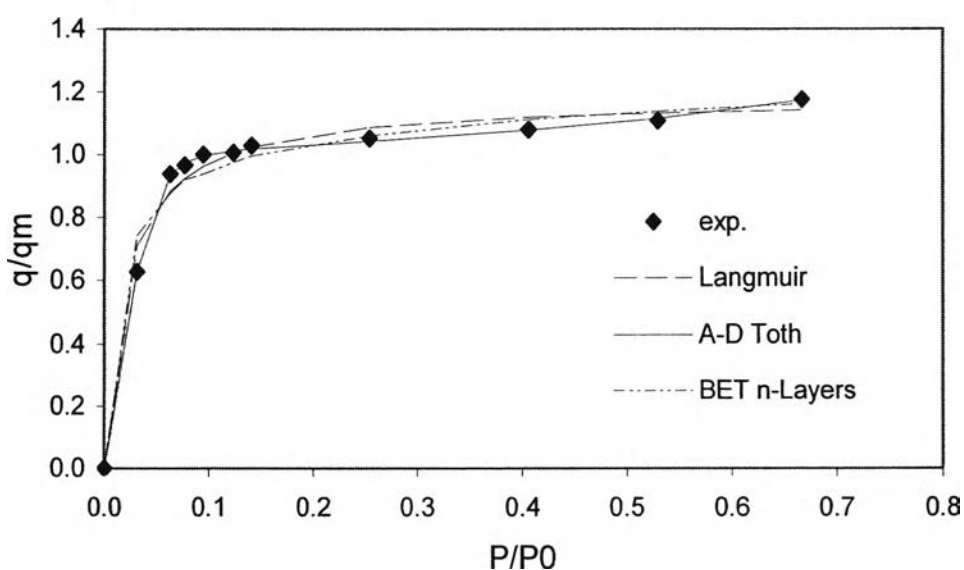


Figure 5.19 Equilibrium dsorption isotherm of fresh 1/16'' molecular sieve zeolite.

The A-D for Toth isotherms also gave the best fit with the experimental data with $r^2 = 0.999$ as shown in Table 5.12.

Table 5.12 Comparison of the equilibrium adsorption isotherm equations for fresh molecular sieve zeolite of size 1/16''

Isotherm	Equilibrium adsorption isotherm equation [†]
Langmuir	$q^* = \frac{q}{q_m} = \frac{9.848c}{1 + 0.47264c}, r^2 = 0.984$
A-D for Toth	$q^* = \frac{q}{q_m} = \frac{P}{(1.889 \times 10^{14} + P^{2.867})^{\frac{1}{2.867}} (1 - P/P_s)^{0.14405}}, r^2 = 0.998$
BET for n-Layers	$q^* = \frac{q}{q_m} = \left[\frac{86.3429(P/P_s)}{1 - (P/P_s)} \right] \left[\frac{1 - (1.4219 + 1)(P/P_s)^{1.4219} + 1.4219(P/P_s)^{1.4219+1}}{1 + (86.3429 - 1)(P/P_s) - 86.3429(P/P_s)^{(1.4219+1)}} \right], r^2 = 0.975$

[†] q = moles adsorbed, q_m = moles adsorbed at complete monolayer, c = concentration (mol/l), P = pressure (kPa), P_s = saturated pressure (kPa)

5.3.2 The Equilibrium Adsorption isotherms of Deactivated Adsorbents

As mentioned in the adsorbent characterization part that the adsorption capacities of deactivated adsorbents were decreased when the adsorbents deactivated, so the shape of the adsorption isotherm of deactivated adsorbents can be change, which leads to the change of the adsorption isotherm equation at each deactivation condition. The equilibrium adsorption isotherms of all prepared deactivation cases were developed and discussed in this part.

5.3.2.1 Deactivated Alumina

The experimental adsorption isotherm of deactivated alumina indicates that the water vapor still adsorbs as multilayer, which can be explained by Freundlich equation, although the adsorption ability was decreased as seen in Figure 5.20. In addition, the adsorption behavior of deactivated alumina changes to slow adsorption of water at low relative humidity and then to rapid adsorption at around 30-40 percentages of relative humidity. The adsorption isotherm equations were developed and shown in Table 5.13.

Table 5.13 Equilibrium adsorption isotherm equations of fresh and deactivated alumina

%Deactivation*	Equilibrium adsorption isotherm equation ^r		r ²
0 (Fresh)	Freundlich	$q^* = 1.195c^{0.8313}$	0.999
42.46	Freundlich	$q^* = 0.29311c^{1.082}$	0.991
67.92	Freundlich	$q^* = 0.02018c^{1.661}$	0.976
77.97	Freundlich	$q^* = 0.01452c^{1.699}$	0.962
88.30	Freundlich	$q^* = 0.0161c^{1.623}$	0.955

* %deactivation due to the loss of adsorption capacity

^r q = adsorption capacity (g water/100 g of adsorbent), c = concentration (mol/l)

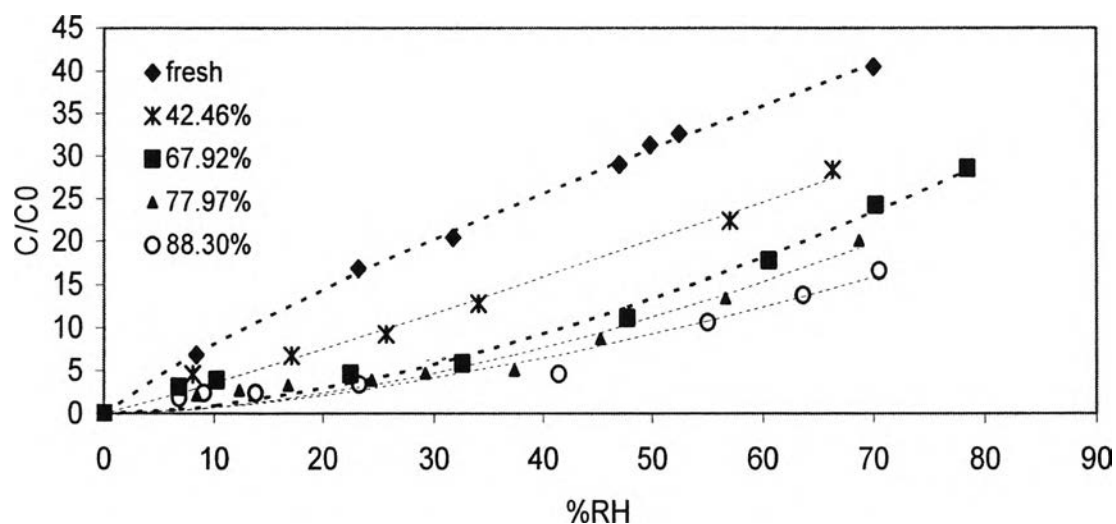


Figure 5.20 The equilibrium adsorption isotherms of activated alumina of fresh, 42.5, 67.9, 78.0, and 88.3% deactivation due to loss of their adsorption capacity.

5.3.2.2 Deactivated Molecular Sieve Zeolite

The adsorption behavior of deactivated zeolite is the same as of the fresh one, but the lower adsorption capacity was observed. Therefore, the A-D equations were also applied for their equilibrium adsorption isotherms, but the constants in the equation were changed to appropriate values.

A. Deactivated 1/8" Molecular Sieve Zeolite

The adsorption behavior of deactivated 1/8" molecular sieve zeolite explained by the A-D equations is shown in Table 5.14.

Table 5.14 Equilibrium adsorption isotherm equations of fresh and deactivated 1/8" molecular sieve zeolite

%Deactivation*	Equilibrium adsorption isotherm equation [†]	r ²
0 (fresh)	$q^* = \frac{q}{q_m} = \frac{P}{(5.423 \times 10^{10} + P^{2.173})^{\frac{1}{2.173}} (1 - P/P_s)^{0.1036}}$	0.997
10.81	$q^* = \frac{q}{q_m} = \frac{P}{(3.535 \times 10^{20} + P^{3.774})^{\frac{1}{3.774}} (1 - P/P_s)^{0.07055}}$	0.998
15.13	$q^* = \frac{q}{q_m} = \frac{P}{(3.214 \times 10^{24} + P^{4.155})^{\frac{1}{4.155}} (1 - P/P_s)^{0.03446}}$	0.997

* %deactivation due to the loss of adsorption capacity

[†] q = moles adsorbed, q_m = moles adsorbed at complete monolayer, P = pressure (kPa), P_s = saturated pressure (kPa)

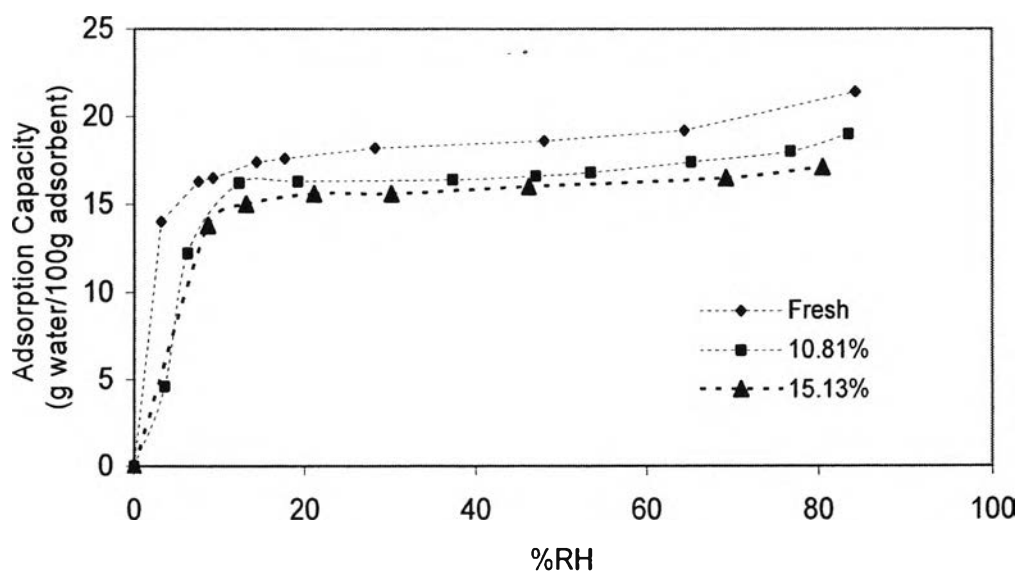


Figure 5.21 The equilibrium adsorption isotherms of 1/8" molecular sieve zeolite at several percentages of deactivation by the loss of their adsorption capacity.

The experimental equilibrium adsorption isotherms of 10.81 and 15.13% deactivated adsorbents indicate that the complete monolayer adsorption capacity changes from 17.5 to 16.3 g of water /100g of fresh adsorbent and to 15.7 g of water /100g for 10.81% and 15.13% deactivated adsorbent, respectively, as shown in Figure 5.21.

B. Deactivated 1/16" Molecular Sieve Zeolite

The equilibrium adsorption isotherms of deactivated 1/16" molecular sieve zeolite appear in the same tend as of the 1/8" one. The isotherm equations are shown in Table 5.15.

Table 5.15 Equilibrium adsorption isotherm equations of fresh and deactivated 1/16" molecular sieve zeolite

%Deactivation*	Equilibrium adsorption isotherm equation [†]	r ²
0 (fresh)	$q^* = \frac{q}{q_m} = \frac{P}{(1.889 \times 10^{14} + P^{2.867})^{\frac{1}{2.867}} (1 - P/P_s)^{0.14405}}$	0.997
5.79	$q^* = \frac{q}{q_m} = \frac{P}{(1.666 \times 10^{18} + P^{3.6121})^{\frac{1}{3.6121}} (1 - P/P_s)^{0.05738}}$	0.989
14.10	$q^* = \frac{q}{q_m} = \frac{P}{(3.843 \times 10^{21} + P^{4.1745})^{\frac{1}{4.1745}} (1 - P/P_s)^{0.06396}}$	0.997

* %deactivation due to the loss of adsorption capacity

[†] q = moles adsorbed, q_m = moles adsorbed at complete monolayer, P = pressure (kPa), P_s = saturated pressure (kPa)

The experimental equilibrium adsorption isotherms of 5.79% and 14.11% deactivated adsorbents indicate that the complete monolayer adsorption capacity changes from 17.7 to 17.0 g of water /100g of fresh adsorbent and to 15.8 g of water/100 g for 5.79% and 14.10% deactivated adsorbent, respectively, as shown in Figure 5.22.

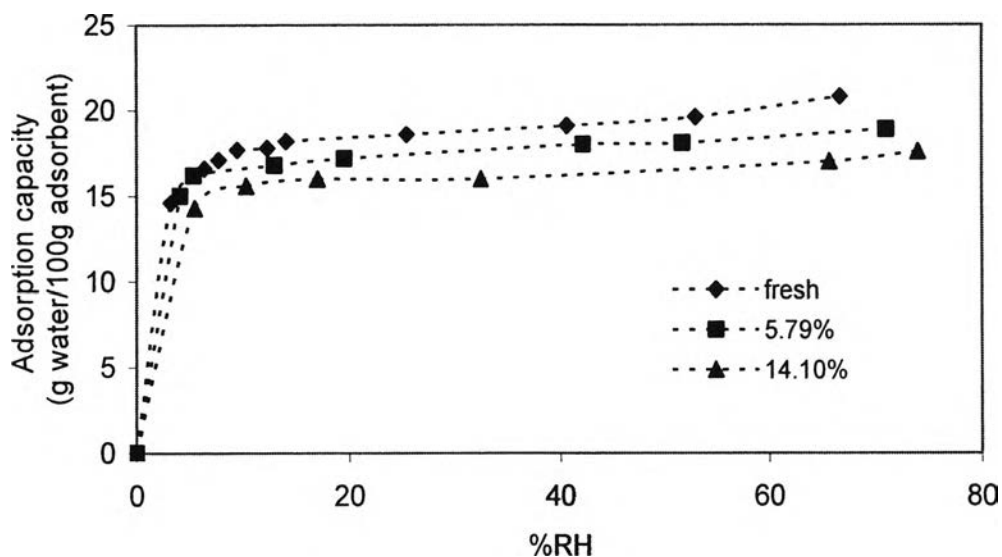


Figure 5.22 The equilibrium adsorption isotherms of 1/16'' molecular sieve zeolite at several percentages of deactivation by the loss of their adsorption capacity.

5.3.3 Correlation of Constants in Equilibrium Adsorption Isotherm with Degree of Deactivation

5.3.3.1 *Activated Alumina*

The equilibrium adsorption behavior of fresh and deactivated alumina can be explained by Freundlich equation. All constants of fresh and deactivated equilibrium adsorption isotherm equations of alumina are listed in Table 5.16.

Table 5.16 Values of all constants in the equilibrium adsorption isotherm equations of fresh and deactivated alumina

%Deactivation	Parameters	
	Freundlich ($q^*=ac^b$)	
	a	b
0	1.195	0.8313
42.5	0.2931	1.082
67.9	0.02018	1.661
78.0	0.01452	1.699
88.3	0.01610	1.623

The relationship between the constants (“a” and “b”) in the Freundlich equation and deactivation is shown in Figure 5.23. The plot implies that the constant “a” is continually decreased until the alumina deactivated up to 70%, after that it is stable. For the constant “b”, it is gradually increased until the deactivation reaches around 70%. Then, it keeps steady.

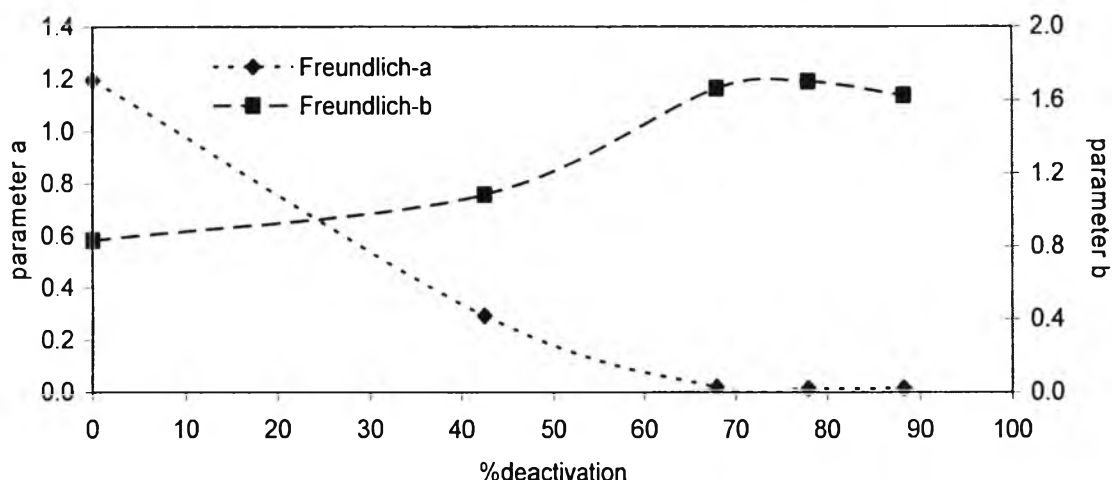


Figure 5.23 Relationship between the constants a and b in the Freundlich equations and degree of deactivation of alumina.

Since “a” is the Freundlich adsorption constant, the decrease of “a” means the adsorption ability of water vapor on the alumina surface is decreased when the alumina is deactivated. Also, the increase of constant “b” means the water vapor molecules tend to adsorb on each other due to the lack of the active alumina surface. In addition, at the degree of deactivation over 70%, the adsorption capacity is found to be quite stable as discussed in the adsorbent characterization part. This is confirmed by the steadiness of constant “a” and “b” as shown in Figure 5.23.

5.3.3.2 Molecular Sieve Zeolite

As the A-D for Toth equation can explain the behavior of all deactivated molecular sieve adsorption for all the range of relative humidity, the relationship of each parameter and deactivation can be plotted. Table 5.17 shows all parameters in the A-D equations for the fresh and deactivated molecular sieve zeolites.

Table 5.17 Values of all constants in the A-D equations of the fresh and deactivated molecular sieve zeolite

Adsorbent	%deactivation	Parameters		
		A-D for Toth ($q^*=P/((b+Pt)^{1/t}(1-P/P_0)^d)$)		
		b	t	d
1/8" molsiv	0	5.42E+10	2.173	0.10362
	10.81	3.53E+20	3.774	0.07055
	15.13	3.21E+24	4.155	0.03446
1/16" molsiv	0	1.89E+14	2.867	0.14405
	5.79	1.67E+18	3.612	0.05738
	14.11	3.84E+21	4.175	0.06396

Figures 5.24 to 5.26 exhibit the plot of each constant, "b", "t", and "d" in the equilibrium adsorption isotherm equations of molecular sieve zeolite versus several deactivation percentages. These plots exhibit the increase of "b" and "t", but "d" is decreased. The decrease of constant "d" while the molecular sieves deactivate, eventually results in the disappearance of the term $(1-P/P_0)^d$. Then, the adsorption behavior described by the A-D for Toth equation becomes to be only the Toth equation, which the increase of "b" and "t" consequently means the amount of monolayer capacity is decreased.

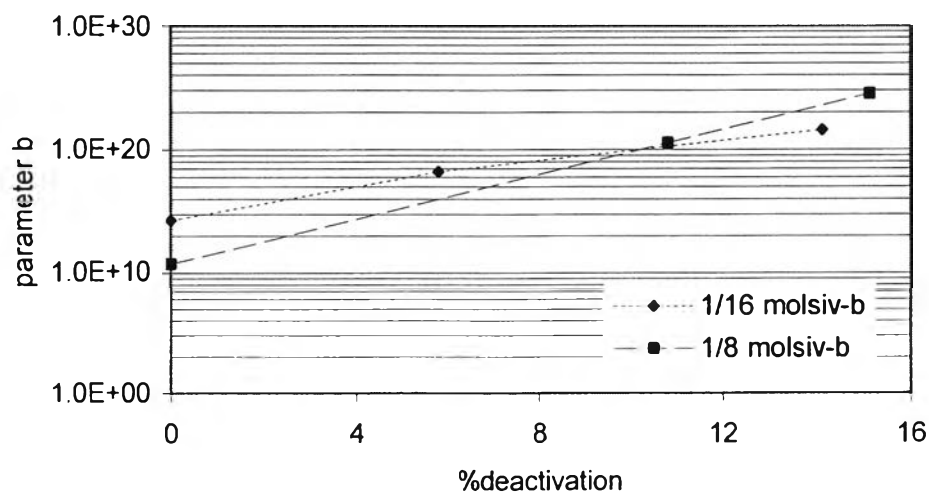


Figure 5.24 Relationship between the constant b in the A-D for Toth equations of the 1/8" and 1/16" molecular sieve zeolite and degree of deactivation.

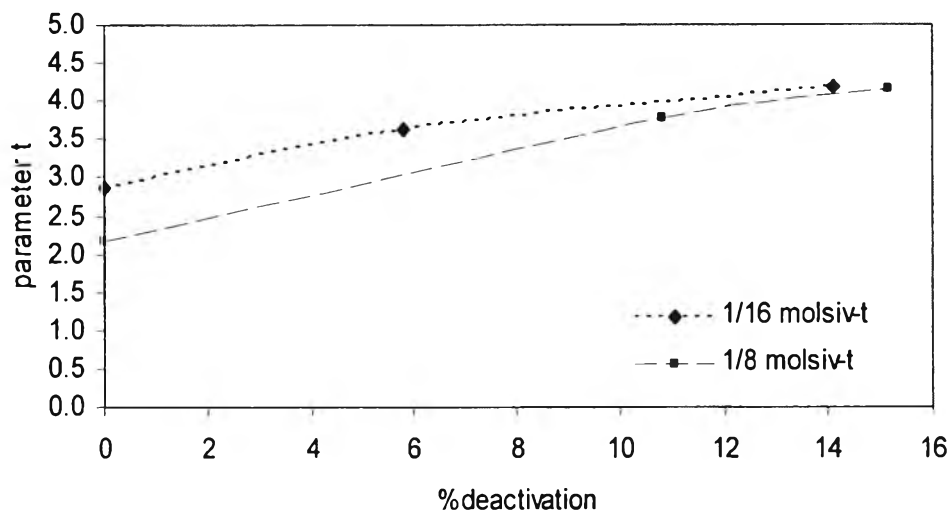


Figure 5.25 Relationship between the constant t in A-D for Toth equations of the 1/8" and 1/16" molecular sieve zeolite and degree of deactivation.

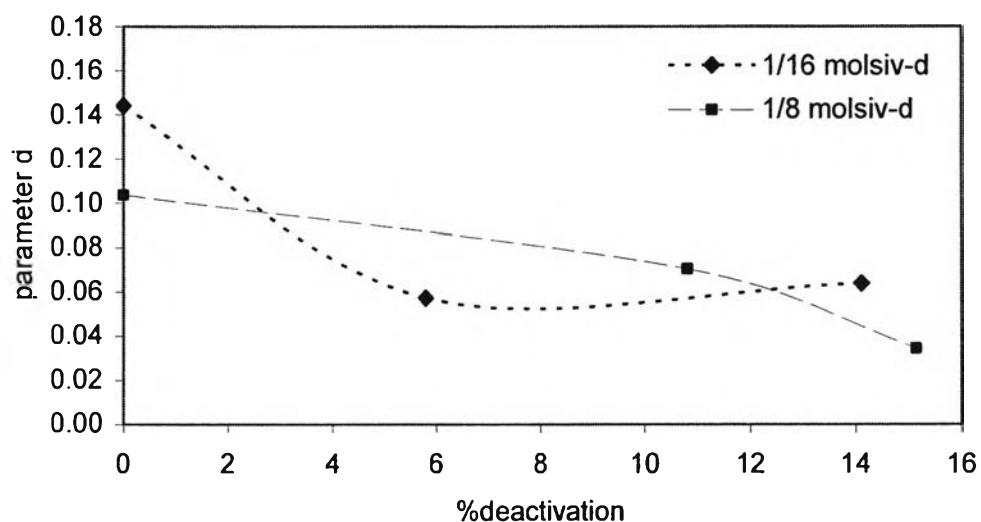


Figure 5.26 Relationship between the constant d in A-D for Toth equations of the 1/8" and 1/16" molecular sieve zeolite and degree of deactivation.

5.4 Experimental Breakthrough Curves

In this work, the dynamics of a fixed-bed adsorber was studied to obtain the water breakthrough curves. The deactivation of the adsorbents packed in the adsorber was investigated for its effect on the breakthrough curve, and the outcomes were compared to that of the fresh bed. The experiments for breakthrough curve

determination were carried out with the feed concentration of 30%RH and the fixed contact time of 9.83 seconds. The packed layers are shown in Appendix D.

5.4.1 Experimental Breakthrough Curve of Fresh Fixed-bed Adsorber packed with All Fresh Adsorbents

The wet natural gas at 30%RH was fed to the adsorber with the flow rate of 457.8 ml/min, and the relative humidity level at the outlet of the adsorbent was monitored until the breakthrough curve was completed. The breakthrough curve for the fresh bed packed with the fresh adsorbents is shown in Figure 5.27. For this operating condition, the breakthrough time (the time consumed at the point where the water concentration of the effluent begins to appear) is about 27.8 hours.

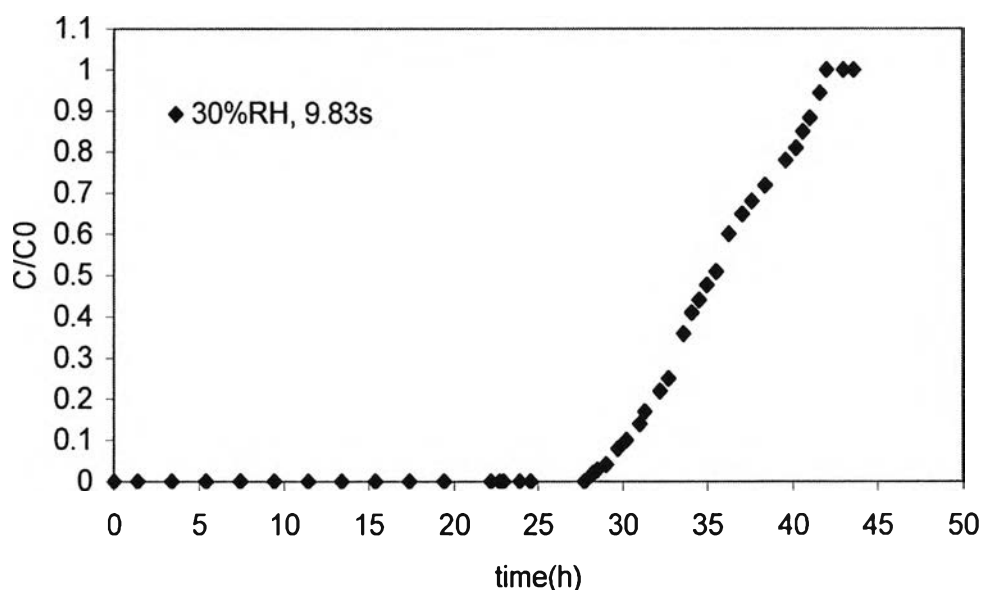


Figure 5.27 Experimental breakthrough curve of the fresh bed packed with the fresh adsorbents (the inlet water concentration of 30%RH and the contact time of 9.83s).

5.4.2 Experimental Breakthrough Curve of Fixed-bed Adsorber packed with Deactivated Adsorbents

The dynamics of the adsorber packed with 88.3% deactivated alumina, 15.13% deactivated 1/8" molsiv, and 14.10% deactivated of 1/16" molsiv in a multilayer fashion was also studied at the same condition as the fresh bed packed with the fresh adsorbents. The experimental breakthrough curve was developed, and

the water concentration breakthrough occurs around 24 hours as shown in Figure 5.28.

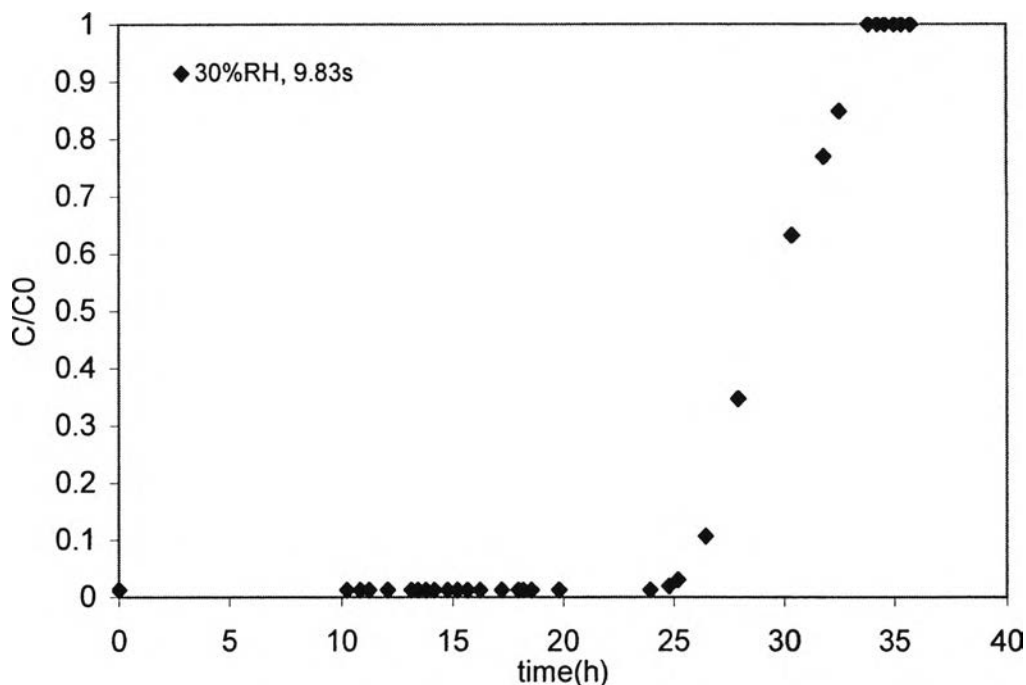


Figure 5.28 Experimental breakthrough curve of the bed packed with 88.3% deactivated alumina, 15.13%deactivated 1/8" mol siv, and 14.10% deactivated molsiv (the inlet water concentration of 30%RH, and the contact time of 9.83s).

Figure 5.28 indicates the breakthrough time of the fixed-bed packed with the deactivated adsorbents is shorter when compared with the one packed with all fresh adsorbents.

5.5 Theoretical Breakthrough Curve

The mathematical model for prediction of experimental breakthrough time developed by Chaikasetpaiboon (2002) and Uttamaroop (2003) was used in this part. It is based on the assumption of an axially dispersed pug flow, isothermal system, constant fluid velocity, and no pressure drop. The physical properties and the equilibrium adsorption isotherm of each adsorbent were employed in the mathematical model. The parameters applied in modeling are shown in Appendix E.

5.5.1 Comparison of Experimental and Theoretical Breakthrough Curves of Fixed-bed packed with Fresh Adsorbents

The predicted breakthrough profiles for water adsorption on the multilayer adsorber at the same conditions of experiment are demonstrated in Figure 5.29. The breakthrough time predicted from the model using $k = 8.5 \times 10^{-5} \text{ s}^{-1}$ is about 25 hours accounted for 6.47% error from the experiment.

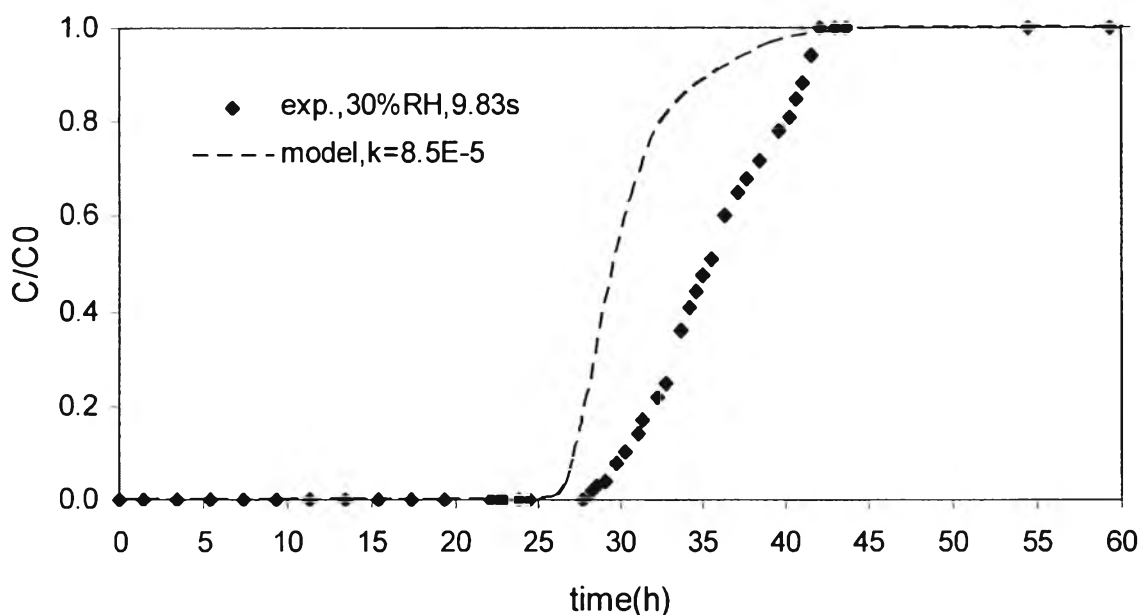


Figure 5.29 Comparison between the experimental and theoretical breakthrough curves at the contact time of 9.83 sec and the feed humidity of 30%RH.

The sensitivity analysis on the overall mass transfer coefficient affecting to the shape of the breakthrough curve was also studied in this part, as similar as in Uttamaroop (2003). The results showed that the increase of overall mass transfer coefficient resulted in steeper breakthrough curve. The sensitivity of k value is described in Appendix G.

5.5.2 Comparison of Experimental and Theoretical Breakthrough Curves of Fixed-bed packed with Deactivated Adsorbent

The equilibrium adsorption isotherms of deactivated adsorbents were applied in the mathematical model to predict the breakthrough profile of a deactivated bed at the same conditions. When the molecular sieve zeolites were deactivated the pellets were destroyed and their crystal sizes were decreased, thus the void fractions for both molecular sieves were corrected in the model (Appendix H). From the best fit, the breakthrough time is around 22 hours, and gives about 8.3% difference when compared to the experimental data as shown in Figure 5.30.

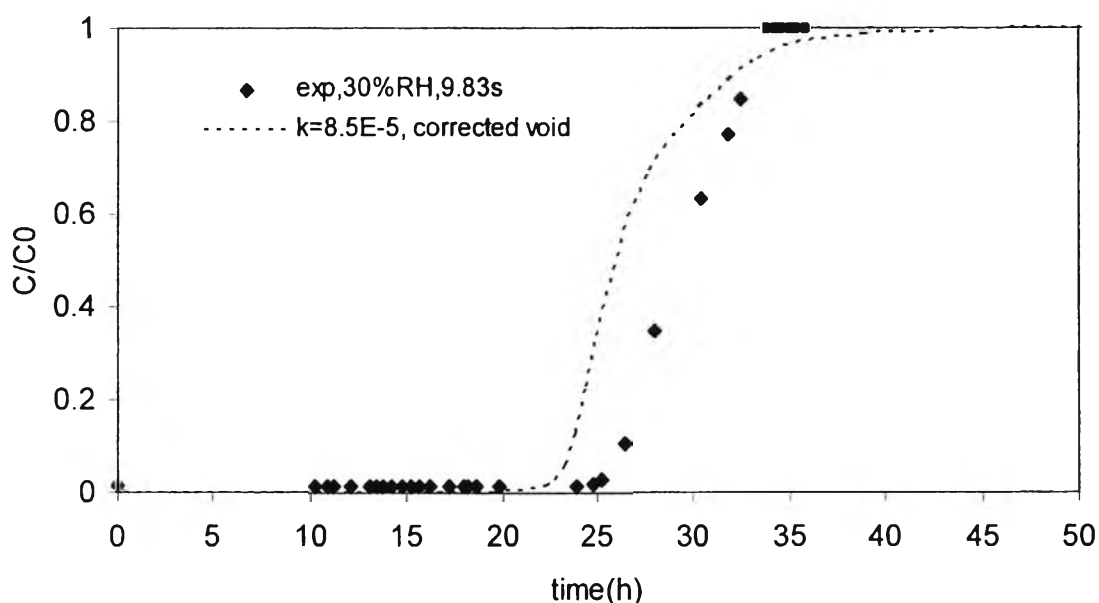


Figure 5.30 Comparison between experimental and theoretical breakthrough curves of fixed-bed adsorber packed with 88.3% deactivated alumina, 15.13% deactivated 1/8" molsiv, and 14.10% deactivated molsiv at the contact time of 9.83 sec and the feed humidity of 30%RH.

5.6 Predicted Breakthrough Time of Multi-Layer Deactivated Adsorbents

The theoretical breakthrough time changed by deactivation of the adsorbents was predicted for all possible beds packed with the adsorbents with various degrees of deactivation. The multi-layer adsorber contains alumina on the top, followed by the 1/8" molecular sieve, and the 1/16" molecular sieve in the

bottom. Table 5.18 illustrates the notation used in this part to represent adsorbents at various degrees of deactivation.

Table 5.18 Notation for adsorbents at various degrees of deactivation

Material	%Deactivation	Deactivation ratio	Activity*	Notation
Alumina	0	0	1	F _A
	42.46	0.42	0.58	D _{1A}
	67.92	0.68	0.32	D _{2A}
	77.97	0.78	0.22	D _{3A}
	88.30	0.88	0.12	D _{4A}
Molsiv (1/8")	0	0	1	F _{UIB}
	10.81	0.11	0.89	D _{1UIB}
	15.13	0.15	0.85	D _{2UIB}
Molsiv (1/16")	0	0	1	F _{UIS}
	5.79	0.58	0.94	D _{1UIS}
	14.10	0.14	0.86	D _{2UIS}

* activity (a_t) = observed adsorption capacity at time t / adsorption capacity at time t = 0

The deactivation of each layer of packed bed adsorber can directly affect to the breakthrough time. As the adsorption ability of deactivated adsorbents is less than that of the fresh one, the life time of deactivated adsorbents should also be shorter. The results in Table 5.19 show the effect of deactivation in each layer on the theoretical breakthrough time of the adsorber, so the sensitivity of the deactivated adsorbents in each layer will also be discussed later. Then, the theoretical breakthrough time ratio in Table 5.19 was plotted versus deactivation ratio as shown in Figure 5.31. This figure is developed based on figure 4.3 in approach 2.

The results exhibit that the deactivation rate of alumina was the fastest, and from the calculation, it was found that at 10% deactivation, the alumina deactivated by 6.3 times of 1/8" molecular sieve and 3.2 times of 1/16" molecular sieve. Although alumina is the easiest deactivated material, but its deactivation does not affect much to the breakthrough time. In contrast, the theoretical breakthrough time extremely decreased in the case of deactivated 1/8" molecular sieve. This means the breakthrough time is sensitive to the deactivation for the 1/8" molecular sieve.

Table 5.19 The theoretically predicted breakthrough time of several sets of deactivated beds

Description	Multi-layer bed	Breakthrough time(h)*	Breakthrough time ratio**
All fresh adsorbents	$F_A F_{UIB} F_{UIS}$	26	1
Deactivated alumina, fresh Molsiv Zeolites	$D_{1A} F_{UIB} F_{UIS}$	24.9	0.96
	$D_{2A} F_{UIB} F_{UIS}$	24.9	0.96
	$D_{3A} F_{UIB} F_{UIS}$	24.8	0.95
	$D_{4A} F_{UIB} F_{UIS}$	24.8	0.95
Fresh alumina, Deactivated 1/8" molsiv, and Fresh 1/16" Molsiv	$F_A D_{1UIB} F_{UIS}$	23.1	0.89
	$F_A D_{2UIB} F_{UIS}$	20.5	0.79
Fresh alumina, Fresh 1/8" molsiv, and Deactivated 1/16" Molsiv	$F_A F_{UIB} D_{1UIS}$	24.8	0.95
	$F_A F_{UIB} D_{2UIS}$	23.9	0.92

*at 30%RH natural gas feed and 9.83s contact time

** Breakthrough time ratio = breakthrough time of a deactivated bed / breakthrough time of fresh bed

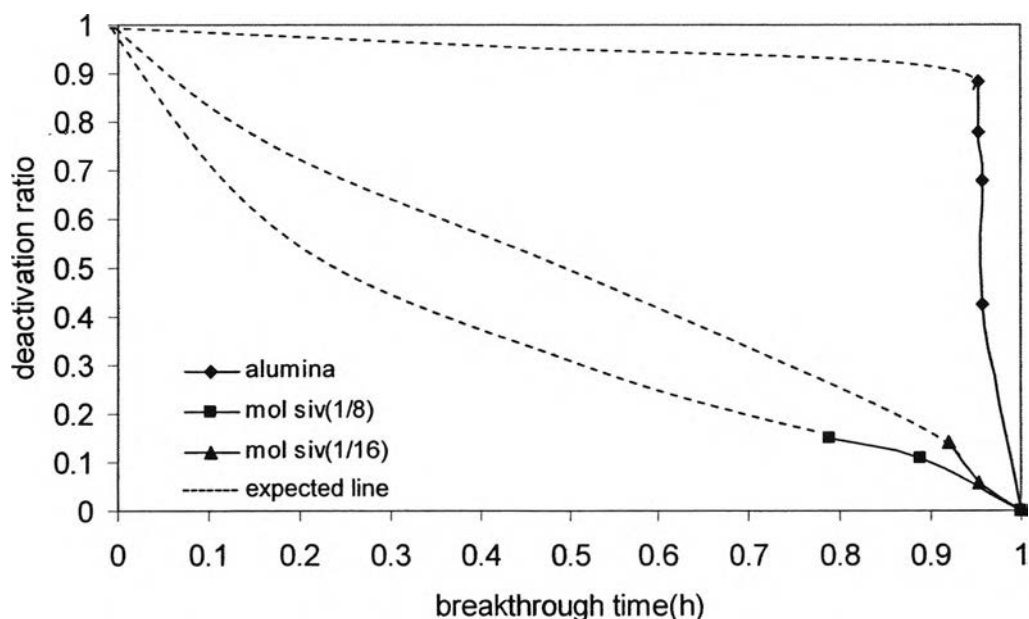


Figure 5.31 Relationship of deactivation ratio and theoretical breakthrough time ratio for each adsorbents.

The use of Figure 5.31 is to indicate the deactivation percentages or activity of each adsorbent remained in the packed bed at each of several breakthrough time measurements. If the relationship between the real operating time and the activity could be developed, and the deactivation rate of each adsorbent could be obtained and employed in the mathematical model of the multilayer adsorber, the mathematical modeling in association with deactivation of adsorbents as proposed in Approach 1 in Chapter IV could be completed.

However, some sensitive parameters, such as void fraction and axial dispersion coefficient were kept constant upon various degrees of deactivation for each layer. So, the theoretical breakthrough times displayed in this part were subjected to these limitations. However, the trend of change could be representative.

Not only was the effect of each layer studied, but the theoretical breakthrough time changed by deactivation of adsorbents for all possible cases were also studied. Since the activated alumina is easily deactivated, it tends to be the first adsorbent deactivated among the others in the adsorber. The breakthrough time in the case when the alumina layer was deactivated by 42.5% and 88.3 % combined with all cases of other layers are shown in Table 5.20 and 5.21, respectively.

Table 5.20 Predicted breakthrough time of the adsorber packed with 42.5% deactivated alumina (D_{1A}) on the top and the Molsiv adsorbents with various degrees of deactivation in the bottom

Alumina	Molsiv (1/8")	Molsiv (1/16")	Breakthrough time(h)
F_A	F_{UIB}	F_{UIS}	26.0
D_{1A}	F_{UIB}	F_{UIS} ↓	24.9
D_{1A}	F_{UIB}	D_{1UIS} ↓	24.6
D_{1A}	F_{UIB}	D_{2UIS} ↓	23.9
D_{1A}	D_{1UIB}	F_{UIS} ↓	23.7
D_{1A}	D_{1UIB}	D_{1UIS} ↓	23.9
D_{1A}	D_{1UIB}	D_{2UIS} ↓	23.0
D_{1A}	D_{2UIB}	F_{UIS} ↓	22.8
D_{1A}	D_{2UIB}	D_{1UIS} ↓	22.6
D_{1A}	D_{2UIB}	D_{2UIS} ↓	22.3

* Note: See the explanation of each notation in the Table 5.18

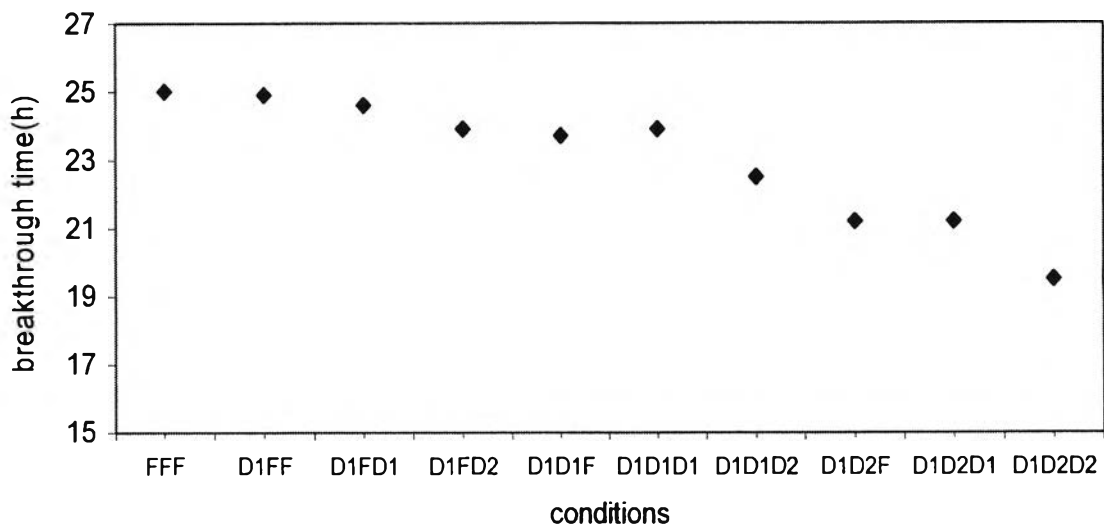


Figure 5.32 Predicted breakthrough time of the adsorber packed with 42.5% deactivated alumina (D_{1A}) on the top and the Molsiv adsorbents with various degrees of deactivation in the bottom.

Figures 5.32 and 5.33 exhibit the breakthrough time of all possible beds presented in Table 5.19 and 5.20, respectively.

Table 5.21 Predicted breakthrough time of the adsorber packed with 88.3% deactivated alumina (D_{2A}) on the top and the Molsiv adsorbents with various degrees of deactivation in the bottom

Alumina	Molsiv (1/8")	Molsiv (1/16")	Breakthrough time(h)
F_A	F_{UIB}	F_{UIS}	26.0
D_{4A}	F_{UIB}	F_{UIS} ↓	24.8
D_{4A}	F_{UIB}	D_{1UIS} ↓	24.8
D_{4A}	F_{UIB}	D_{2UIS} ↓	23.8
D_{4A}	D_{1UIB}	F_{UIS} ↓	23.2
D_{4A}	D_{1UIB}	D_{1UIS} ↓	23.2
D_{4A}	D_{1UIB}	D_{2UIS} ↓	22.9
D_{4A}	D_{2UIB}	F_{UIS} ↓	22.5
D_{4A}	D_{2UIB}	D_{1UIS} ↓	22.2
D_{4A}	D_{2UIB}	D_{2UIS} ↓	22.0

* Note: See the explanation of each notation in the Table 5.18

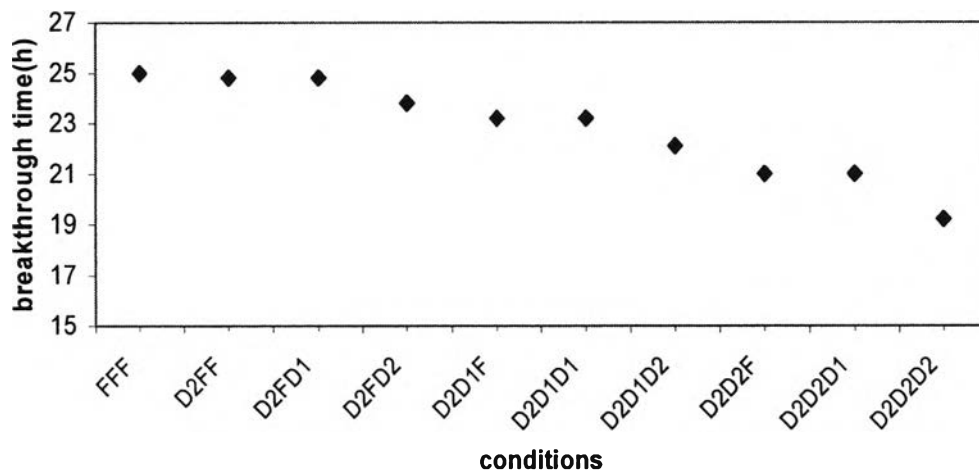


Figure 5.33 Predicted breakthrough time of the adsorber packed with 88.3% deactivated alumina (D_{2A}) on the top and Molsiv adsorbents with various degrees of deactivation in the bottom.